

# Multicanonical Study of Continuum Physics in the D=2 $O(3)$ Nonlinear Sigma Model

**T. Neuhaus**

FB8 Physik, BUGH Wuppertal, Germany

October 19, 2018

## **Abstract**

Employing a variant of the Multicanonical Ensemble we study twisted spin configurations on periodic boxes in the  $D = 2$   $O(3)$  nonlinear sigma model for  $\beta$ -values inbetween 1.55 to 3.1. The free energy difference of twisted spin configurations is determined from the constraint effective potential. The finite size scaling behavior is in accordance with the asymptotically free nature of the continuum theory. Upon certain reasonable assumptions we determine the  $\Delta\beta(\beta)$ -shift of the stiffness correlation length  $\xi_s$ . The mass-gap as determined by our analysis is  $m_0 = 79.6(1.9) \Lambda_{latt}$ . This value agrees with the analytical result of the thermodynamic Bethe Ansatz  $m_0 = 80.1 \Lambda_{latt}$ .

# 1 Introduction

The two dimensional  $O(3)$  nonlinear sigma model is a asymptotically free field theory [1]. It deserves special interest in view of asymptotically free four dimensional nonabelian gauge theories describing the strong interactions inbetween Quarks. A fundamental feature of these theories is the existence of a nonvanishing mass-gap  $m_0$ . Recently the mass-gap of the sigma model has been calculated analytically on the basis of the thermodynamic Bethe Ansatz [2, 3]. Choosing the simplest regulator, namely a two dimensional hypercubic lattice with lattice spacing  $a$ , and the standard nearest neighbor action functional with nearest neighbor coupling  $\beta$  we consider

$$S = -\beta \sum_{\langle i,j \rangle} \phi_i^\alpha \phi_j^\alpha, \quad (1)$$

where the fields  $\phi_i^\alpha$  are 3-component unit vectors and the sum  $\langle i, j \rangle$  runs over the nearest neighbors on the lattice. The mass-gap correlation length  $\xi_0 = m_0^{-1}$  has the value

$$\xi_0^{theor} = a \frac{e^{1-\pi/2}}{8} \frac{e^{2\pi\beta}}{2^{5/2}} \frac{1}{2\pi\beta} \left(1 - \frac{.091}{\beta} + O(1/\beta^2)\right), \quad (2)$$

corresponding to the exact mass gap  $m_0 = 80.0864 \Lambda_{latt}$  [3],  $\Lambda_{latt}$  denoting the 3-loop lattice cut-off parameter [4]. The past numerical studies of the path integral [5, 6] consistently overestimated this number. These studies considered infinite volume mass-gap correlation length values  $\xi_0$  up to about hundred lattice spacings  $a$  with the help of cluster algorithms. It was also attempted to enlarge the accessible correlation length region utilizing real space renormalization group methods [5]. It was found, that asymptotic perturbative scaling only sets in at mass-gap correlation length values, which can hardly be fitted into the memory of todays computers. In addition it may also be appropriate to mention the still standing criticism of Patrascioiu, Seiler and others on the continuum limit of the sigma model [7]. These authors argue in favor of a the existence of a phase with vanishing mass-gap in the sigma model, which is however not supported by the numerical data [8]. It is therefore a challenge to confront the known analytical result on the mass-gap with the precision numerical simulations of the path integral. From such a study we might also gain better insight on how to accurately determine the mass-gap of lattice QCD.

Finite size scaling theory [9] has been very successful throughout the years in predicting the behavior of the infinite volume correlation length of spin systems at criticality from the properties of finite systems, which in this paper are taken to be square boxes with linear extent  $L$  and periodic boundary conditions. In a situation where the control parameter  $x_0 = \xi_0/L$  is large and, even at the critical point, where the correlation length is infinite, the path integrals singular part of the free energy on finite volume systems is a function of the control parameter  $x_0$  alone. The Fisher scaling analysis leads to reliable determinations of the correlation length divergence critical exponent  $\nu$  in statistical mechanics models.

In this paper we attempt a generalization of this idea to the  $D = 2$  nonlinear sigma model. Its asymptotic freedom fixed point is located at infinite value of the bare nearest neighbor coupling. The quantity under consideration is a free energy difference of twisted relative to untwisted spin configurations - the spin stiffness - forming a Bloch wall, whose finite size scaling behavior is dominated by logarithmic terms in the control parameter  $x_s = \xi_s/L$  in accord with the perturbative treatment of the path integral in the one-loop approximation. The quantity  $\xi_s$  hereby denotes the stiffness correlation length. We will argue, that a precise extraction of the  $\Delta\beta(\beta)$ -shift corresponding to the stiffness correlation length is feasible up to  $\beta$ -values as large as 3.1, upon reasonable assumptions on the coefficients of the finite size scaling law. The integration of the shift in junction with a start value for the mass-gap correlation length  $\xi_0$  allows the determination of the mass-gap  $m_0$ . The paper is organized as follows: Section 2 is devoted to the theoretical background and introduces the constraint effective potential, the considered free energy difference and discusses the finite size scaling hypothesis. Section 3 contains details of the Multicanonical Ensemble simulation. In section 4 we present our numerical analysis and results. Section 5 concludes the of the paper.

## 2 Theoretical Considerations

In statistical field theories, which share the universality class of continuous ferromagnets, it is well known on the basis of the  $\epsilon$ -expansion and the renormalization group [10], that the critical behavior of the system can be studied in the symmetry broken phase of the theory by considering path integrals of configurations, which interpolate inbetween regions of different order pa-

parameter orientation. The helicity modulus  $Y$  carries the information on the nonanalytical behavior in the symmetry broken phase of the theory. It is common to define the helicity modulus by the response of the system with respect to a twist angle  $\Theta$ , which is applied microscopically to the fields on the boundary of the lattice in one of the lattice directions. Denoting  $F = -\ln Z$  the free energy, the free energy difference

$$\Delta F_Y(\theta) = F(\theta) - F(\theta = 0) \quad (3)$$

then defines the helicity modulus [11]

$$Y = \lim_{(\Omega, L) \rightarrow \infty} \frac{2L}{\theta^2 \Omega} \Delta F_Y(\Theta), \quad (4)$$

which is finite in the thermodynamic limit and allows for a geometry independent i.e.,  $\Theta$ -independent, characterization of the Bloch wall. Hereby denotes  $\Omega$  the cross section orthogonal to the direction of the twist. E. g., on a hypercubic lattices with linear extent  $L$  one has  $\Omega \propto L^{D-1}$  and one expects  $\Delta F_Y(\theta) \propto L^{D-2}$ . The critical behavior of the theory in terms of the helicity modulus is expressed by Josephsons scaling law [12]:  $Y = A_Y t^{\mu_J}$  with  $\mu_J = (D - 2)\nu$ . It is clear, that the presented scaling laws refer to the ferromagnetic case. In fact, when the dimension  $D = 2$  is approached from above for field theories with continuous symmetry, like the  $O(N)$  nonlinear sigma model with  $N \geq 3$ <sup>1</sup>, the ferromagnetic character of the theory is lost and the helicity modulus  $Y$  according to eq.(4) vanishes for any value of the bare coupling  $\beta$ . In dimension  $D = 2$  the infinite volume system exhibits domains of different order parameter orientations, which are free to fluctuate. This is the content of the Mermin Wagner theorem.

At the heart of the problem is a study of the correspondingly defined free energy difference  $\Delta F_s(\Theta)$  on finite lattices in the  $D = 2$   $O(3)$  nonlinear sigma model at large values of the nearest neighbor coupling i.e., in a situation in which the mass-gap correlation length  $\xi_0$  exceeds the linear extent  $L$  of the symmetric hypercubic lattice. In this situation one expects  $\Delta F_s(\Theta)$  to be controlled by  $x_s = \xi_s/L$ , where  $\xi_s$  denotes the stiffness correlation length. Based on the renormalization group, the  $\epsilon = D - 2$ -expansion and the 1-loop approximation, the calculation has been performed for the case of a continuum square box with fixed twisted boundary conditions [13, 14]. We

---

<sup>1</sup>We refrain from a discussion of the  $O(2)$  symmetric XY model.

quote the result

$$\Delta F_s(\Theta) = \frac{\Theta^2}{4\pi} [\ln(\xi_s/L) + \ln \ln(\xi_s/L)] + R(\Theta) + \mathcal{O}(\infty). \quad (5)$$

A few remarks are in order:

1) According to the expected Fisher scaling  $\Delta F_s(\Theta)$  splits into a singular part, which is a function of  $x_s = \xi_s/L$  alone and a regular contribution  $R(\Theta)$ . The stiffness correlation length  $\xi_s$  follows the perturbative renormalization group, and thus in the large  $\beta$ -limit has the form

$$\xi_s(\beta) \propto \frac{1}{\beta} e^{2\pi\beta}. \quad (6)$$

However,  $\xi_s$  is not identical to the mass-gap correlation length  $\xi_0$  as is the control parameter  $x_s$  as compared to  $x_0$ . The stiffness correlation length  $\xi_s$  describes the crossover of the system from its small volume behavior at large values of  $x_s$  into a state of various domains of order parameter orientation on large volumes. It is expected to be larger than the mass-gap correlation length  $\xi_0$ . Recently Billoire performed a high statistics numerical calculation of the stiffness correlation length [15] at  $\beta$ -values far in the perturbative region  $\beta = 5, 10$  and  $20$  respectively. Expressing the measurement in units of the exact mass-gap correlation length we quote  $\xi_s = 9.39(1), 9.46(1)$  and  $9.47(1)\xi_0^{theor}$ . In this paper we assume  $\xi_s$  takes its perturbative value that at a  $\beta$ -value of  $3$ . In addition we expect a region of  $\beta$ -values, where  $\xi_s$  as well as  $\xi_0$  are governed by the same beta-shift  $\Delta\beta(\beta)$ . Let us denote with  $\Delta\beta(\beta)$  the change of the coupling  $\beta$  to  $\hat{\beta} = \beta - \Delta\beta(\beta)$  corresponding to the decrease of the stiffness correlation length by a factor of  $2$ :  $\xi_s(\hat{\beta}) = \frac{1}{2}\xi_s(\beta)$ .

2) The free energy difference  $\Delta F_s(\Theta)$  at  $\Theta = 0$  defines the  $\Theta$  independent spin stiffness  $\rho = \frac{2}{\Theta^2} \Delta F_s(\Theta)$ . The large  $\beta$  perturbative limit of  $\rho_s = -\frac{\partial}{\partial \ln L} \rho$  defines the spin stiffness constant whose value is  $\frac{1}{2\pi}$ . Precision numerical simulations of the spin stiffness [15, 16] confirm this theoretical expectation. In the context of the present paper we assume that the spin stiffness coefficient proportional to  $\ln L$  takes its perturbative value in the whole considered  $\beta$  region.

3) Upon insertion of eq.(6) into eq.(5) we observe, that the leading term in  $\Delta F_s$  is  $\beta\Theta^2/2$ . This is the classical action difference of a twisted configuration at twist angle  $\Theta$  relative to a configuration with twist angle  $\Theta = 0$ . The dominant effects of quantum fluctuations at fixed  $\beta$  are linear in  $\ln L$  and are

given by a term  $-\Theta^2 \ln L / 4\pi$ . They drive the spin stiffness to smaller values on the larger system sizes, as expected.

4) The regular contribution  $R(\Theta)$  in eq.(5) can be calculated in the small  $\Theta$  expansion. For the boundary conditions considered in [14] one finds [15]  $R(\Theta) = -2.501 \frac{\Theta^4}{8\pi^4} + \mathcal{O}(\Theta^6)$  i.e., a negative contribution at finite  $\Theta$  values. We note that these contributions are nonuniversal in character and depend on the details of the implementation of the twist.

Numerical simulations of free energies are computationally difficult. In the standard approach one integrates the expectation value of the action difference of systems with nonzero twist  $\Theta$  and twist  $\Theta = 0$  along the nearest neighbor coupling parameter direction  $\beta$ . One can avoid the integration of the action by differentiating the path integral with respect to  $\Theta$  at a value of  $\Theta = 0$  [15, 17]. In this paper we consider the constraint effective potential (CEP) [18] of the mean field of the theory.

The consideration of the CEP is motivated by the analogous problem arising in the interfacial case in  $Z(2)$  symmetric theories and recently numerical simulations of it have been conducted with the help of Multicanonical Ensemble simulations [19]. One considers the mean field  $M = \frac{1}{L^D} \sum_i S_i$  of the Ising fields. Its probability distribution  $P(M)$  contains at the same time the information concerning bulk as well as interfacial properties of the system. Relevant for interfacial effects are states at  $M = 0$  on finite boxes with periodic boundary conditions. In this region of the phase space configurations contain two domains of opposite order parameter orientation and two interfaces are formed. Widoms scaling law can be analyzed [20]. Lee and Kosterlitz have performed a finite size scaling analysis of the CEP at criticality [21] leading to a determination of  $\nu$ .

In case of the theory with continuous  $O(3)$  symmetry we introduce the 3-component field

$$\Phi^\alpha = \frac{1}{L^2} \sum_x \phi_x^\alpha \quad (7)$$

and its absolute value, denoted the mean field  $\bar{\Phi}$  in the following

$$\bar{\Phi} = \sqrt{\sum_\alpha \Phi^\alpha \Phi^\alpha}, \quad (8)$$

which will have the probability distribution

$$P(\bar{\Phi}) \propto \bar{\Phi}^2 e^{-U(\bar{\Phi})} \quad (9)$$

in the canonical ensemble of the theory. The function  $U(\bar{\Phi})$  is the CEP of the theory. It can be obtained by rewriting the partition function

$$Z = \int D\phi e^{\beta \sum_{x,\nu} \phi_x^\alpha \phi_{x+\nu}^\alpha} \quad (10)$$

into

$$Z = \int_0^\infty d\bar{\Phi} \bar{\Phi}^2 e^{-U(\bar{\Phi})}, \quad (11)$$

which can be achieved by introducing suitable  $\delta$ -functions and integration upon the remaining degrees of freedom. We note that  $U(\bar{\Phi})$  is defined up to constant, which can easily be absorbed into a multiplicative normalization of  $Z$ . In addition a factor  $\bar{\Phi}^{N-1}$  at  $N = 3$  appears in the path integral definition of  $U$ . This factor is proportional to the surface of a  $N$ -sphere of radius  $\bar{\Phi}$  and accounts for the degeneracy of states with respect to  $O(N)$  rotations. Without taking this phase factor properly into account the CEP is a singular function at  $\bar{\Phi} = 0$ .

The CEP attracted in the past attention in the context of the Higgs-models represented by  $O(N)$  symmetric theories in  $D = 3$  and  $D = 4$ . There it was studied with analytic methods [22] as well with numerical simulations [23]. In these models the CEP has at a finite value  $\bar{\Phi}_{min}$  a minimum, which corresponds to the Higgs field expectation value. We may note, that both analytic, as well as the numerical considerations in these models were concerned with the shape of the CEP in the vicinity of its minimum.

In the context of the present paper we are however concerned with the CEP at values of the mean field  $\bar{\Phi}$  equal to  $\bar{\Phi} = 0$ . We argue that states at  $\bar{\Phi} = 0$  correspond on hypercubic boxes with periodic boundary conditions to Bloch walls carrying formally a twist angle of  $\Theta = 2\pi$ . This can be easily seen on the classical level by noting, that the field configuration

$$\phi^1 = \cos\left(\frac{2\pi n_1}{L}\right) \quad \phi^2 = \sin\left(\frac{2\pi n_1}{L}\right) \quad \phi^3 = 0 \quad (12)$$

minimizes the action functional for the given periodic boundary conditions at  $\bar{\Phi} = 0$ . This configuration exhibits on the scale of one lattice spacing  $a$  spin twists of value  $\frac{2\pi}{L}$  in the 1-direction of the lattice, which upon integration in the 1-direction adds up to a total twist angle of  $\Theta = 2\pi$ . We expect this configuration and the added quantum fluctuations to dominate the  $\bar{\Phi} = 0$  state. Thus in the framework of the CEP it is strongly suggested, that the

singular part of  $\Delta F_s(\Theta = 2\pi)$  exhibits the same finite size scaling as the constraint effective potential difference, or potential barrier

$$\Delta U = U(\bar{\Phi} = 0) - U(\bar{\Phi}_{min}) = \Delta F_s(\Theta = 2\pi) + \hat{R}, \quad (13)$$

up to regular terms  $\hat{R}$ , provided the CEP exhibits a maximum and minimum corresponding to the twisted and untwisted states. It is this finite size scaling hypothesis, which we will examine in the subsequent analysis of this paper. We will find, that the numerical evaluation of the CEP confirms the hypothesis.

### 3 The Multicanonical Ensemble Simulation

By the use of standard Monte Carlo algorithms it would be very difficult to sample values of  $\bar{\Phi}$  close to zero, if the value of the nearest neighbor coupling  $\beta$  is larger than about 1.6 on lattices of reasonable linear size  $L$ . To overcome this difficulty, we modify the importance sampling by introducing a Multicanonical-weight factor into the Monte Carlo sampling process [19]. We remark, that the idea of Multicanonical Ensemble simulations consists in modifying the Boltzmann-weight for the purpose of the improvement of the actual Monte Carlo sampling process. The modification is however done in such a way, that the effect of the Multicanonical-weight will be removed in a well controlled way. Thus in the end the CEP can be determined in the canonical ensemble of the theory.

In case of the CEP the Multicanonical-weight factor is chosen to be a function of the mean field  $\bar{\Phi}$  evaluated on each single configuration and will be denoted  $W_{mc}(\bar{\Phi})$ . It is in principal defined on the real interval  $[0, L^2]$  and it is sensible to split the Multicanonical-weight into a part, which takes care of the degeneracy with respect to  $O(3)$  rotations, and a yet unknown contribution  $\hat{W}_{mc}(\bar{\Phi})$ . Thus for the purpose of the Monte Carlo simulation we consider the Multicanonical-weight

$$W_{mc}(\bar{\Phi}) = -2 \ln \bar{\Phi} + \hat{W}_{mc}(\bar{\Phi}) \quad (14)$$

and

$$e^{-S+W_{mc}(\bar{\Phi})} \quad (15)$$

to be the Boltzmann-factor, which generates the Markov process. In order to obtain a representation of the Multicanonical-weight  $\hat{W}_{mc}$ , which in a



computer is easily calculable, we choose  $\hat{W}_{mc}$  to be a polygon, which on a finite set of  $i = 1, m$  intervals  $I_i : \bar{\Phi}_i \leq \bar{\Phi} < \bar{\Phi}_{i+1}$  for each interval is characterized by two parameters  $g_i$  and  $h_i$ :

$$\hat{W}_{mc}(\bar{\Phi}) = g_i + h_i \bar{\Phi}. \quad (16)$$

One may view the parameters  $h_i$  as magnetic sources, which are applied on piecewise intervals of the operator  $\bar{\Phi}$  to the theory. In one of our earlier publications we therefore named the resulting ensemble the Multimagnetical Ensemble [20]. We found it sufficient in the actual numerical simulations, to first determine a value  $\bar{\Phi}_{max}$  in a standard simulation. In this situation  $\bar{\Phi}_{max}$  is calculated in such a way, that all the relevant structure of the CEP, namely the location of its minimum, and the states at  $\bar{\Phi} = 0$  are included in the considered  $\bar{\Phi}$ -interval. It means that we will only evaluate the shape of the CEP for values  $0 \leq \bar{\Phi} \leq \bar{\Phi}_{max}$ . We then choose for reasons of simplicity an aequidistant partition of the considered  $\bar{\Phi}$ -interval into  $m = 25$  or  $m = 40$  different intervals  $I_i$ , which in the actual simulations turned out to be a sufficiently fine polygon approximation to the Multicanonical-weight  $\hat{W}_{mc}$ .

Multicanonical Ensemble simulations are defined by the requirement, that the considered operator exhibits an almost constant, ideally a constant, probability distribution in the simulation. If in the canonical ensemble the density of states function with mean field  $\bar{\Phi}$  is denoted  $n(\bar{\Phi})$ , then the ideal Multicanonical-weight factor is

$$W_{mc}(\Phi_0) = -ln n(\bar{\Phi}). \quad (17)$$

Though trivial, we note, that a priori the Multicanonical-weight is not known. Less trivial we remark, that it is possible to obtain an estimate of the weight factor from the Monte Carlo simulation. In the vicinity of a given value of the operator  $\bar{\Phi}$  one may sample the phase space in an attempt to estimate the density of states. In practice we perform for each of the considered intervals  $I_i$  a separate simulation with  $\bar{\Phi}$ -values constrained to the given interval. In the simulation each parameter  $h_i$  is then determined under the requirement that the probability distribution of the mean field  $\bar{\Phi}$  approximates the Multicanonical distribution at its best. The full set of all parameters  $h_i$  serves the purpose of the construction of the complete Multicanonical-weight according to eq.(14) and eq.(15). Clearly, for given  $h_i$  the parameters  $g_i$  can be chosen in such a way, that the resulting polygon is a steady function of  $\bar{\Phi}$ . We note, that one parameter value, e.g.  $g_1$  is left undetermined by this

procedure. This again corresponds to the overall normalization freedom of the path integral. In our actual simulations we have found, that this simple and robust procedure results into acceptable Multicanonical-weights and distribution functions.

Once the Multicanonical-weight factor has been determined, we implement one sweep of the Monte Carlo sampling by a combination of a Swendsen-Wang reflection cluster update [24, 25], followed by a subsequent accept-reject decision, which then depends on  $W_{mc}$  alone. It means, that we define the Cluster degrees of freedom from the kinetic term of the action, and, that we replace the usual equal probability rule of the Cluster update, by a 4-hit Metropolis accept-reject decision in all the Cluster degrees of freedom, depending on the magnetic properties of the system. At this value for the number of hits we obtained average acceptance rates for moves of the system at about one half for almost all the considered  $\beta$  and  $L$  values. In order to monitor the performance of this update procedure, we divided the considered  $\bar{\Phi}$ -interval into an arbitrarily chosen 8, but equally spaced bins. We measure the average flip-autocorrelation time  $\tau_f$  for a transition of the system from the first to the eighth bin, or vice versa. While due to the partitioning some arbitrariness in the definition of  $\tau_f$  is induced, we nevertheless expect, that it will exhibit the basic aspects of the Monte Carlo time dynamics. Fig. 1) contains data for the quantity  $\tau_f$  obtained on a  $L = 36$  lattice for  $\beta$ -values in between 1.6 and 3.0 (circles), and for a fixed  $\beta$ -value  $\beta = 2.4$  on lattice sizes ranging in between  $L = 20$  to  $L = 68$  (triangles). One notices a typical time scale of several thousand sweeps, which in general is characteristic for our simulation. In detail we observe, that at a given  $\beta$ -value the flip-autocorrelation time stays almost constant, or even decreases with increasing lattice sizes. We attribute this favorable property to the nonlocal nature the algorithm. We also observe on the given lattice a rapid increase of the flip-autocorrelation time with increasing  $\beta$ . Such an increase is expected, as the simulational complexity of the theory will rise in the proximity of the asymptotic freedom fixed point.

In the Multicanonical simulation we measure the Multicanonical probability distribution  $P_{mc}(\bar{\Phi})$  of the mean field  $\bar{\Phi}$ . It is related to the probability distribution in the canonical ensemble  $P(\bar{\Phi})$  by a simple reweighing step

$$P(\bar{\Phi}) \propto P_{mc}(\bar{\Phi}_0)e^{-W_{mc}(\bar{\Phi})} \quad (18)$$

and thus with the help of eq.(9) the CEP can be determined in the Multicanonical simulations. Throughout our simulations we have fixed the mini-

mum value of the CEP to be zero. In addition we perform a bias corrected jackknife error analysis for all the measured quantities. The typical statistics accumulated for each data point in our simulation was inbetween 1 and 5 megasweeps, depending on the considered  $\beta$ -value.

## 4 Numerical Analysis and Results

The mass-gap correlation length  $\xi_0$  of the  $D = 2$   $O(3)$  nonlinear sigma model has been calculated in previous studies at not too large values of  $\beta$  and we quote here the results of Wolff [6]: At the  $\beta$ -values  $\beta = 1.6, 1.7, 1.8$  and  $1.9$   $\xi_0/a$  takes the values  $19.07(06), 34.57(07), 64.78(15)$  and  $121.2(6)$  respectively. In this paper we study small systems of sizes ranging in between  $L = 8$  up to  $L = 82$ . For  $\beta$ -values larger than  $\beta = 1.6$  the mass-gap correlation length  $\xi_0$  is comparable with the considered lattice sizes. Accordingly it is expected that the stiffness correlation length  $\xi_s$  exceeds the linear size of the systems and the onset Fisher scaling may be expected. In a first set of simulations we have studied the  $L$ -dependence of the CEP at twelve values of the nearest neighbor coupling, namely at the  $\beta$ -values  $\beta = 1.6, 1.7, 1.8, 1.9, 2.0, 2.1, 2.2, 2.3, 2.4$  and at the  $\beta$ -values  $\beta = 2.6, 2.8$  and  $\beta = 3.0$ . In a second set of simulations the  $\beta$ -dependence of the CEP potential was determined on a  $L = 36$  lattice at  $\beta$ -values ranging inbetween  $\beta = 1.55$  up to  $\beta = 3.1$ . In total we have accumulated 468 pairs of couplings  $\beta$  and lattice sizes  $L$  within our simulation.

It is important to check our basic assumption, that states at mean field  $\bar{\Phi} = 0$  carry a twist angle of  $\Theta = 2\pi$ . For this purpose we use a special graphical representation of the field configuration, which is exhibited in Fig. 2a) and Fig. 2b). On the given configuration we apply in a first step a global rotation which equals the arbitrarily chosen 3 component of the field  $\Phi^\alpha$  to zero. We then map the 1 and 2 components of the fields along paths in the lattice onto the complex plane. In this mapping we connect fields, which are neighbors within the path, by a line. Fig. 2a) contains all such mappings, which are obtained by considering all  $L$  paths along the main axis of the lattice in the 1-direction. Fig. 2b) contains the analogous graphs for paths along the main axis in the 2-direction. The considered lattice size is  $L = 36$  and the nearest neighbor coupling is  $\beta = 8$ , far in the perturbative region. The value of  $\bar{\Phi}$  for the considered configuration was  $\bar{\Phi} = 0.003904$ , which is very close to zero. One clearly observes the winding angle of  $2\pi$  for the

latter case i.e., for all paths on the main axis of the lattice in the 2-direction, which is clear evidence in favor of the above assumption. It is noteworthy to remark that fluctuations around the classical state eq.(12) are sizable even for such a large  $\beta$ -value. They increase as  $\beta$  is lowered and decrease as  $\beta$  is enlarged. In addition we also mention, that states at  $\bar{\Phi} = 0$  apparently break the cubic group lattice symmetry i.e., in the here considered configuration the twist appears in the 2-direction of the lattice. We have checked, that statistical independent configurations at  $\bar{\Phi} = 0$  assume the possible different twist directions with equal probability. From a theoretical point of view it must be expected that this additional degree of freedom, as compared to a theory with a fixed direction of the twist, contributes to the unknown regular contributions of the finite size scaling relation eq.(13).

In Fig. 3a) and Fig. 3b) we display the CEP, as obtained by our simulations on lattice sizes  $L = 24, 36$  and  $L = 70$  and at a values of  $\beta = 1.6$  and  $\beta = 2.4$ .

At  $\beta = 1.6$  we observe a crossover from a situation, where for the smaller  $L$ -values the CEP for states at  $\bar{\Phi} = 0$  exhibits a barrier  $\Delta U > 0$ , to a situation at the largest  $L$ -value, where the barrier vanishes. Thus the decrease of the spin stiffness with increasing  $L$  is observed. This is attributed to the quantum fluctuations around the classical state with twist angle  $\Theta = 2\pi$ . We may remark, that in simulations of ferromagnets, namely the  $D = 3$   $O(3)$  sigma model in its symmetry broken phase, we have witnessed an increase of the potential barrier with increasing  $L$ .

At  $\beta = 2.4$  the mass-gap correlation length and  $\xi_s$  exceed the linear lattice size by a large factor. Correspondingly a crossover cannot be observed and  $\Delta U \approx 20$  is finite on the considered range of lattice sizes. Again its decrease with increasing  $L$  is witnessed. The large value of  $\Delta U$  corresponds to an exponentially large suppression of states with mean field  $\bar{\Phi} = 0$ , even if the phase space factor of eq.(9) is divided out from the probability distributions. In fact, a simulation of the  $D = 2$   $O(3)$  nonlinear sigma model at  $\beta = 2.4$  on small volumes resembles, as far as order parameter orientation is concerned, on the first sight the behavior of a ferromagnetic system. It is only, that on lattices with linear extent comparable and larger to  $\xi_s$ , the system will approach its true vacuum state.

From the shape of the CEP we have carefully determined the quantity  $\Delta U = U(\bar{\Phi} = 0) - U(\bar{\Phi}_{min})$ . For this purpose we employ fits to the shape of the CEP in the vicinity of the minimum at  $\bar{\Phi}_{min}$  and in the vicinity of  $\bar{\Phi} = 0$ . In the vicinity of  $\bar{\Phi} = 0$  and for the determination of  $U(\bar{\Phi} = 0)$  we

describe the CEP by a parabola. Such a functional form can be expected on the basis of a classical argument

$$U = U(\bar{\Phi} = 0) + \alpha_1 \bar{\Phi}^2 \quad (19)$$

and is consistent with the data. We use it in a fit range of  $\bar{\Phi}$ -values close to  $\bar{\Phi} = 0$ , for which corresponding  $\chi_{d.o.f.}^2$ -values of the fits are smaller than unity. Inspecting the shape of the CEP in vicinity of its minimum we note an apparent asymmetric behavior and therefore we use the form

$$U = U(\bar{\Phi}_{min}) + \beta_1(\bar{\Phi} - \bar{\Phi}_{min})^2 + \beta_2(\bar{\Phi} - \bar{\Phi}_{min})^3 \quad (20)$$

for its analytic description and the determination of  $U(\bar{\Phi}_{min})$ . Analogous remarks as in the previous case on the fit-intervals and the  $\chi_{d.o.f.}^2$ -values apply.

We expect, that discretization effects of the lattice theory, as compared to the continuum, lead to correction terms to the spin stiffness. The leading contributions are of the order  $1/a^2$ . On the lattice and in the classical approximation we calculate the action difference  $\Delta S_{0,latt}$  of a field configuration with twist  $\Theta = 2\pi$  relative to untwisted fields. It has the expansion

$$\Delta S_{0,latt} = \Delta S_{0,c}[\rho(L) + \mathcal{O}(\frac{1}{a^4})], \quad (21)$$

with  $\rho(L)$  given by

$$\rho(L) = 1 - C_g \frac{\pi^2}{3(La)^2}. \quad (22)$$

Classically the constant  $C_g$  is equal to unity, and  $\Delta S_{0,c} = 2\pi^2\beta$  denotes the action difference of the Bloch wall in the continuum. We will assume here, that the possible form of the  $1/a^2$ -corrections is already determined on the classical level. Correspondingly we assume in the fully fluctuating theory, that additional contributions can be accounted for by a nonunity value of the parameter  $C_g$ . The potential barrier in the continuum  $\Delta U_c$  is then related to  $\Delta U$  evaluated on the lattice via the relation

$$\Delta U_c = \rho(L)^{-1} \Delta U, \quad (23)$$

which then allows the comparison of the lattice data with the continuum scaling form.

We have analyzed the finite size scaling of almost all of our  $\Delta U$  data by means of one  $\chi^2$ -fit with the form

$$\Delta U = [1 - C_g \frac{\pi^2}{3(La)^2}] [\pi \ln(\xi_s/L) + A \ln \ln(\xi_s/L) + \tilde{R}]. \quad (24)$$

Aiming at a precise determination of the mass-gap  $\xi_0$  we implement our knowledge about the perturbative limits of the spin stiffness  $\rho$  and the spin stiffness correlation length  $\xi_s$ . We constrain certain parameters and adopt the following scheme:

1) In accord with theoretical expectations the prefactor of the single logarithmic scaling term  $\propto \ln(\xi_s/L)$  of the continuum free energy is fixed to its exact value  $\pi$ . This is expected on the basis of our previous discussion on the spin twist and the spin stiffness. We leave the prefactor  $A$  of the double logarithmic scaling term to be a free parameter. It may be tolerated, that some of the omitted  $\mathcal{O}(1)$  higher order terms of the loop expansion in eq.(24) may be represented effectively by a value of  $A$ , which differs from  $\pi$ .

2) The quantity  $\partial_\beta \ln \xi_s(\beta)$  is expanded in inverse powers of the nearest coupling parameter  $\beta$ . Thus

$$\partial_\beta \ln \xi_s(\beta) = 2\pi - \frac{1}{\beta} + \frac{0.091}{\beta^2} + \sum_{k=3}^6 \gamma_k \frac{1}{\beta^k} \quad (25)$$

represents an analytic form, which incorporates the known 3-loop behavior of the mass-gap correlation length. It is valid, if in the asymptotic scaling region  $\xi_0$  and  $\xi_s$  follow the same  $\beta$  function. Without loss of generality we have included 4 free parameters  $\gamma_k$  for  $k = 3, \dots, 6$ . These additional degrees of freedom allow for deviations from perturbative scaling in the small  $\beta$ -value region, where the dip in the  $\Delta\beta(\beta)$  function is expected.

3) Given a start value for the stiffness correlation length at a value of the nearest neighbor coupling  $\beta^*$  in the perturbative region of the theory,  $\xi_s$  can be integrated to smaller values of  $\beta$  via

$$\ln \xi_s(\beta) = \int_{\beta^*}^{\beta} \partial_\beta \ln \xi_s(\beta) + \ln \xi_s(\beta^*), \quad (26)$$

if within the fit the quantity  $\partial_\beta \ln \xi_s(\beta)$  is represented by its expansion eq.(25). We exploit the recent measurements of the spin stiffness correlation length in the asymptotic scaling region [15] and fix the integration constant  $\ln \xi_s(\beta^*)$  by choosing  $\beta^* = 3$  and  $\xi_s(\beta^*) = 9.47 \xi_0^{theor}(\beta^*)$ . Note then that at  $\beta^* = 3$ ,

$\xi_s$  has a value of  $934051a$ . Any significant deviation of  $\xi_s$  from its measured value in the asymptotic scaling region would appear unreasonable to us at such large values of the correlation length.

4) We also express the functional form for the quantity  $C_g(\beta)$  through an expansion in inverse powers in  $\beta$

$$C_g(\beta) = 1 + \sum_{k=1}^4 \delta_k \frac{1}{\beta^k}, \quad (27)$$

upon introduction of 4 free parameters  $\delta_k$  with  $k = 1, \dots, 4$  parameterizing the departure of  $1/a^2$  corrections from the classical result. At infinite value of  $\beta$  the classical result is recovered.

5) The onset of finite size scaling is expected for large values of the control parameter  $x_s \gg 1$ . Into the actual fit we include data from the  $\beta$ -interval  $1.65 \leq \beta \leq 3.1$ , leaving us with 428 independent data points. For these data and for the considered lattice sizes our final fit only includes data, whose control parameters obey the inequality  $x_s > 4.7$ . Such large values of the control parameter  $x_s$  hopefully put us in a region of the theory, where we can reliably trust our finite size scaling ansatz eq.(24).

The resulting 10 parameter  $\chi^2$ -fit for the parameters  $A, \tilde{R}, \gamma_k$  and  $\delta_k$  with  $k = 1, \dots, 4$  has been executed with the double precision version of the CERN libraries MINUIT program. The error analysis for the parameter values and for all other derived quantities of this paper has been performed by a repeated execution of the fit on several data sets. In each data set any datum in the fit is distributed gaussian around its mean with a variance corresponding to its error. The fit has an excellent  $\chi^2_{d.o.f}$ -value of  $\chi^2_{d.o.f} = 0.75$  and is displayed in Fig. 4) and Fig. 5) in comparison with the measured  $\Delta U$  values. The fit as denoted by the lines in the figures captures the  $\beta$ -dependence of the data in Fig. 4) as well as the  $L$ -dependence displayed in Fig. 5). As expected by the theoretical reasoning the fit supports a negative regular contribution to the scaling law eq.(24)  $\tilde{R} = -3.45(20)$ . It can be compared with the mentioned result of the small  $\Theta$ -expansion of  $\mathcal{O}(\Theta^4)$  on boxes with fixed boundary conditions at a formal value of the twist angle  $2\pi$ , which is  $-5.002$ . However there is no theoretical argument, that both numbers should be identical, rather they should differ by contributions induced by the different boundary conditions. We also find a positive coefficient  $A = 1.79(7)$  attached to the double logarithmic scaling terms. The former value differs from the expected expected value  $\pi$ , which we attribute to the subleading

nature of the double logarithmic terms. In Fig. 6) the fit result for the constant  $C_g$  is given. Finite grid effects are largest for  $\beta$ -values around  $\beta = 1.9$  and exceed their classical value in the constant  $C_g$  by a factor of about 3 there. With increasing  $\beta$  a very slow approach to the classical result is witnessed. In Fig. 7) the logarithm of the stiffness correlation length as well as its  $\beta$ -derivative are displayed. Note again that we have fixed  $\xi_s$  at  $\beta^* = 3$  to the measured perturbative result, the fat circle in the figure. The calculated  $\beta$ -derivative of  $\ln\xi_s$  as displayed by the solid curve in the inlay of Fig. 7) exhibits a very clear "peak like" deviation from 3-loop asymptotic perturbative scaling, the dashed curve in the inlay of Fig. 7). The peak corresponds to the dip in the  $\Delta\beta(\beta)$ -shift as noticed in the earlier studies of the sigma model. It is located at a  $\beta$ -value of about  $\beta \approx 1.75$ . Notably our data demonstrate, that deviations from 3-loop asymptotic scaling are present up to  $\beta$ -values of about  $\beta = 2.5$ , while for all larger values of  $\beta$  asymptotic perturbative scaling is realized within the numerical precision. This finding is a genuine outcome of the present analysis and also applies to the  $\Delta\beta(\beta)$ -shift corresponding to the decrease of the stiffness correlation length by a factor 2. The  $\Delta\beta(\beta)$ -shift is displayed in Fig. 8) for  $\beta$ -values larger than  $\beta = 1.8$ , the solid curve in the figure. It is compared with the 3-loop asymptotic perturbative scaling result, the dashed curve in the figure and with results from Hasenfratz et. al [5]. Table 1) collects few entries for the shift at selected values of  $\beta$ . We thus observe a somewhat slower approach to asymptotic scaling as it was previously anticipated in the numerical simulations. A similar observation has already been reported earlier [26].

The calculation of the mass-gap of the theory in units of the 3-loop lattice cut-off can be attempted under the nontrivial assumption, that mass-gap as well as stiffness correlation length share a common  $\beta$ -value region, in which their flow towards the asymptotically free fixed point with varying couplings is governed by a universal  $\Delta\beta(\beta)$ -shift. In this scaling region the ratio  $\xi_0/\xi_s$  stays constant. It is common believe, that this region stretches beyond the region where asymptotic scaling is observed. Providing a start-value of the mass-gap correlation length at a small value of  $\beta$  outside the perturbative scaling region, but within the so called nonasymptotic scaling region, it may be feasible to integrate the mass-gap of the theory with the help of  $\partial_\beta\xi_s(\beta)$  up to a  $\beta$ -value  $\beta^*$  in the asymptotic scaling region. The existence of a such a universal behavior beyond the asymptotic regime is however by no means guaranteed. Referring to the results of the preceding paragraph we are confident now that the choice  $\beta^* = 3$  moves us into the asymptotic scaling



region. For the start value of the mass-gap correlation length we choose one of Wolffs numbers

$$\xi_0(\beta = 1.8) = 64.78(15)a. \quad (28)$$

This result has been obtained on a quite sizable  $512 \times 512$ -lattice with the help of the cluster algorithm and represents one of the most reliable mass-gap correlation length measurements at large values of the correlation length. It is consistent with another work [5]. In Fig. 9) we display the integration of the mass-gap in units of  $\Lambda_{latt}$  from its start value at  $\beta = 1.8$  up to the largest considered  $\beta$ -values, the solid curve in the figure. We obtain a determination of the mass-gap of the theory in units of the three-loop lattice cut-off parameter

$$m_0 = 79.62 \pm 1.92 \Lambda_{latt}. \quad (29)$$

The quoted error is of statistical nature. This result agrees with the analytical result  $m_0 = 80.0864\Lambda_{latt}$  derived from the thermodynamic Bethe Ansatz.

## 5 Conclusion

The calculation of the mass-gap in the asymptotically free D=2 nonlinear sigma model from the numerical evaluation of the path integral poses a non-trivial problem. In the standard formulation of the theory asymptotic scaling is only exhibited for values of the nearest neighbor coupling  $\beta > 2.5$ . Direct correlation function measurements of the mass-gap are ruled out. A theoretical device is needed in order to connect the small  $\beta$ -region of the theory with the perturbative regime.

In this paper we argue, that the consideration of twisted spin configurations in union with a finite size scaling analysis is able to bridge the gap inbetween the small and large  $\beta$ -regions of the theory. It is possible to determine the coupling parameter flow of the spin stiffness correlation length in a  $\beta$ -interval which connects both regions. Focussing on the theories spin stiffness allows us in addition to adjust certain parameters of the finite size scaling law to their perturbative values. These are obtained either in the numerical simulation or can be given by theoretical arguments. The measured asymptotic value of the spin stiffness correlation length serves as an integration constant for the intgration of  $\xi_s$  towards lower  $\beta$ -values, while the spin stiffness constant  $\rho_s$  adjusts the amplitude of single logarithmic scaling terms of the considered scaling law. This facilitates the precise extraction of

the  $\Delta\beta(\beta)$ -shift corresponding to the nearest neighbor coupling dependence of the stiffness correlation length. Our analysis strongly supports the existence of a scaling window starting at  $\beta$ -values of about 1.8 with an extension into the perturbative scaling regime. Within this region the mass-gap and stiffness correlation length are presumed to flow in coupling parameter space under the rule of a universal  $\Delta\beta(\beta)$ -shift. The integration of the shift in union with a start value for the mass-gap confirms the known theoretical mass-gap result. During the course of our study we have not found any indication in favor of the existence of a phase with vanishing mass-gap in the sigma model. It would be interesting to apply the presented method to twisted gauge field configurations and calculate the mass-gap of lattice QCD.

**Acknowledgments:** The author likes to thank A. Billoire for helpful comments and M. Göckeler for many discussions on the constraint effective potential.

## References

- [1] A. M. Polyakov, Phys. Lett. **B59** (1975) 79; E. Brézin and J. Zinn-Justin, Phys. Rev. Lett. **36** (1976) 691; Phys. Rev. **B14** (1976) 3110.
- [2] P. Hasenfratz and F. Niedermayer, Phys. Lett. **B245** (1990) 529.
- [3] P. Hasenfratz, M. Maggiore and F. Niedermayer, Phys. Lett. **B245** (1990) 552.
- [4] M. Falcioni and A. Treves, Phys. Lett. **B159** (1985) 140; Nucl. Phys. **B265** (1986) 671; S. Caracciolo and A. Pelissetto, Nucl. Phys. **B240** (1994) 141.
- [5] P. Hasenfratz and F. Niedermayer, Nucl. Phys. **B337** (1990) 233, and references therein.
- [6] U. Wolff, Phys. Lett. **B222** (1989) 473; Nucl. Phys. **B334** (1990) 581.
- [7] A. Patrascioiu, Phys. Rev Lett. **58** (1987) 2285; E. Seiler, I. O. Stamatescu, A. Patrascioiu and V. Linke Nucl. Phys. **B305** [FS23] (1988) 623; Phys. Rev. Lett. **60** (1988) 875.
- [8] U. Heller, Phys. Rev. Lett. **60** (1988) 2235; Phys. Rev. D38 (1988) 109; W. Bernreuther and M. Göckeler, Phys. Lett. B214 (1988) 109.
- [9] M. E. Fisher, Rev. Mod. Phys. **46** (1974) 597.
- [10] J. Rudnick and D. Jasnow, Phys. Rev. **B16** (1977) 2032.
- [11] M. E. Fisher, M. N. Barber and D. Jasnow, Phys. Rev. **A8** (1973) 1111.
- [12] B. D. Josephson, Phys. Lett. **21** (1966) 608.
- [13] S. Chakravarty, Phys. Rev. Lett., **66** (1991) 481.
- [14] E. Brézin, E Korutcheva, Th. Jolicœur and J. Zinn-Justin, J. of Stat. Phys., **Vol. 70** (1993) 583.
- [15] A. Billoire in: "Monte Carlo Simulation at very low temperature: The spin stiffness of the 2-D Heisenberg model", Saclay preprint SPhT-95/116.

- [16] M. Caffarel, P. Azaria, B. Delamotte and D. Mouhanna, Europhysics Letters **26** (1994) 493.
- [17] K. K. Mon, Phys. Rev. **B44** (1991) 6809.
- [18] L. O’Raifeartaigh, A. Wipf and H. Yonehama, Nucl. Phys. **B271** (1986) 653.
- [19] B. A. Berg and T. Neuhaus, Phys. Rev. Lett. **68** (1992) 9.
- [20] B. A. Berg, U. Hansmann and T. Neuhaus, Phys. Rev. **B47** (1993) 497; Zeit. f. Phys. B **Vol. 2** (1993) 229.
- [21] J. Lee and J. M. Kosterlitz, Phys. Rev. Lett. **65** (1990) 137.
- [22] M. Göckeler and H. Leutwyler, Phys. Lett. **B253** (1991) 193; Nucl. Phys. **B350** (1991) 228.
- [23] I. Dimitrović, Jürg Nager, K. Jansen and T. Neuhaus, Phys. Lett. **B268** (1991) 408.
- [24] R. H. Swendsen and J. S. Wang, Phys. Rev. Lett **58** (1987) 86.
- [25] F. Niedermayer, Phys. Rev Lett. **61** (1988) 2026; U. Wolff, Phys. Rev. Lett. **62** (1989) 361.
- [26] T. Neuhaus, Nucl. Phys. **B34** ( Proc. Suppl. ) (1994) 667.

## Tables

$\beta$	$\Delta\beta(\beta)$
1.8	.10055(100)
1.9	.10233(051)
2.0	.10598(053)
2.1	.10966(048)
2.2	.11268(044)
2.3	.11486(042)
2.4	.11624(040)
2.5	.11697(038)
2.6	.11724(035)
2.7	.11719(034)
2.8	.11693(034)
2.9	.11655(037)
3.0	.11612(041)
3.1	.11568(046)

Table 1: The  $\Delta\beta(\beta)$ -shift corresponding to changes of the coupling  $\beta$  to  $\hat{\beta} = \beta - \Delta\beta(\beta)$  under the decrease of the stiffness correlation length by a factor of 2 :  $\xi_s(\hat{\beta}) = \frac{1}{2}\xi_s(\beta)$ .

## Figure Captions

**Figure 1:** Flip-autocorrelation time  $\tau_f$  of the Multicanonical Ensemble simulation as defined in section 3 for a fixed  $L = 36$  lattice as a function of  $\beta$  (circles), and at fixed  $\beta = 2.4$  as a function of the linear extent  $L$  (triangles).

**Figure 2:** Graphical representation of a field configuration on a  $36^2$  lattice at vanishing mean field  $\bar{\Phi}$ . The fields on paths are mapped onto the complex plane and neighbors within a path are connected by lines. In Fig. 2a) 36 such mappings are plotted within their corresponding unit circles, if the paths are chosen to be the main axis of the lattice in the 1-direction. Fig. 2b) contains the corresponding mappings, if the paths are chosen in the 2-direction. A winding angle of  $2\pi$  is observed in the latter case. The  $\beta$ -value is  $\beta = 8$ .

**Figure 3:** The CEP on lattices of size  $L = 24$  (circles),  $L = 36$  (triangles) and  $L = 70$  (crosses) at  $\beta = 1.6$  (Fig. 3a)) and at  $\beta = 2.4$  (Fig. 3b)).

**Figure 4:** The quantity  $\Delta U - 2\pi^2\beta$  on a  $36^2$  lattice as function of the coupling  $\beta$ . The inlay displays the quantity  $\Delta U$  without subtraction. The solid curve corresponds to the fit as described in section 4 of the paper. For reasons of simplicity we omit the drawing of error bars, except for one data point.

**Figure 5:** The quantity  $\Delta U$  as a function of  $\ln L$  for 12 selected values of the coupling  $\beta$ . The various curves corresponds to the fit as described in section 4 of the paper. Note that the data at  $\beta = 1.6$  have not been included into the fit. In fact small deviations of the data from the fit become visible for the larger lattice sizes at this value of  $\beta$ . For these data the control parameter  $x_s$  is not large enough.

**Figure 6:** The quantity  $C_g$  as a function of  $\beta$ , the solid curve. The dotted curves indicate the error intervals as supported by the analysis. The dashed horizontal line represents the classical limit.

**Figure 7:** Logarithmic plot of the stiffness correlation length  $\xi_s$ , as obtained in section 4 of the paper. The fat circle corresponds to the start value for  $\xi_s$  in the asymptotic scaling region. The inlay exhibits the  $\beta$ -derivative of  $\ln \xi_s$  characterized by the solid curve. Error intervals are indicated by dotted curves. The dashed curve of the inlay represents the 3-loop perturbative result. The inlay also contains a dotted horizontal line at a value of  $2\pi$ , the constant term in the inverse  $\beta$ -expansion of the considered quantity.

**Figure 8:** The  $\Delta\beta(\beta)$ -shift of the spin stiffness correlation length (solid curve) for values of  $\beta > 1.8$ . The dashed curve again corresponds to the

3-loop perturbative result. Errors intervals are again indicated by dotted curves. The crosses correspond to numerical results of Hasenfratz and Niedermayer, obtained by a real space renormalization group matching procedure.

**Figure 9:** The integration of the mass-gap in units of the lattice cut-off for values of  $\beta > 1.8$ , the solid curve in the plot. Error intervals are treated as before. The dashed horizontal line corresponds the exact result. The start value for the integration is indicated by the solid square. The asymptotic value of the mass-gap is indicated by the solid circle.

FIG. 1

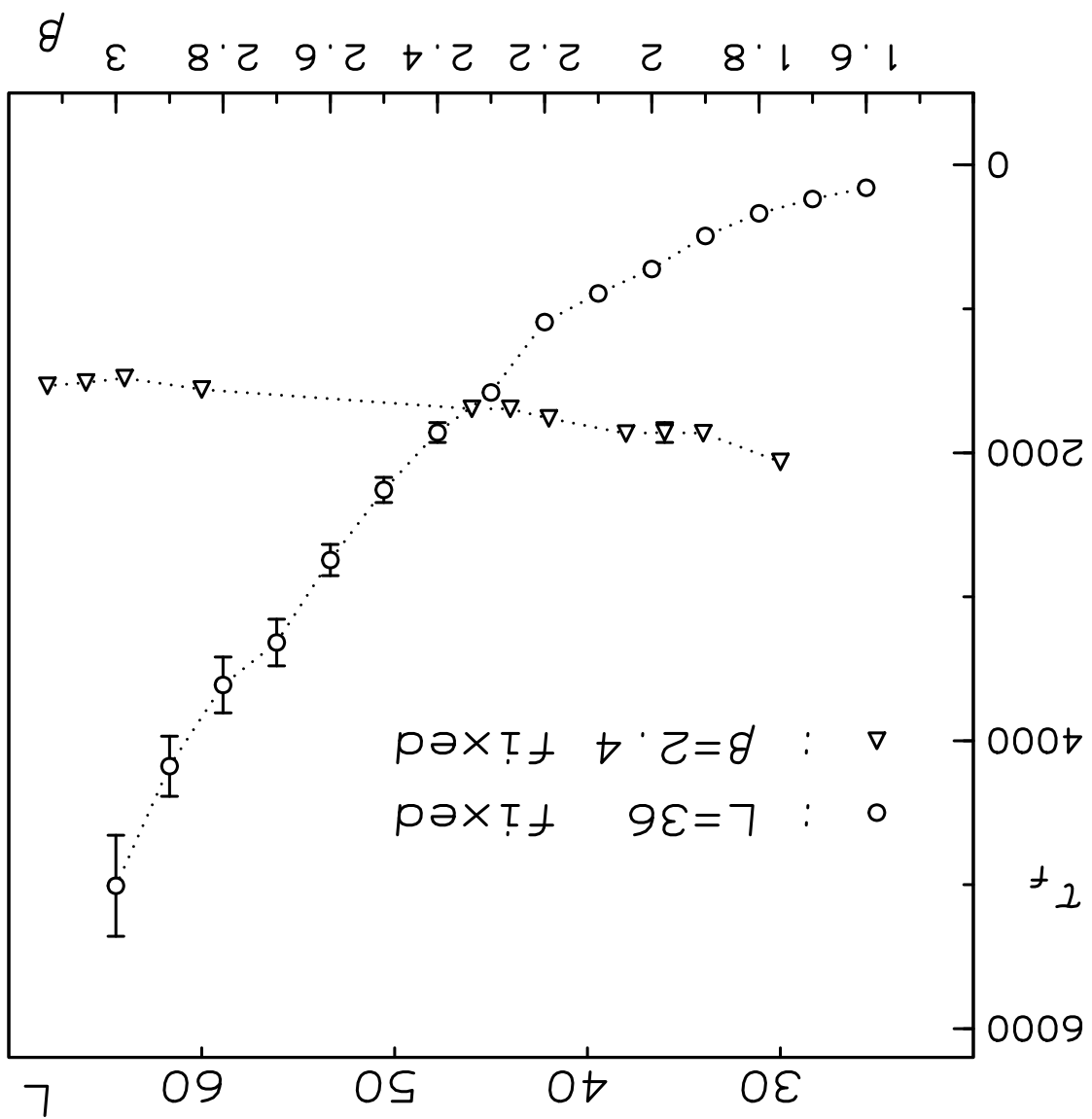
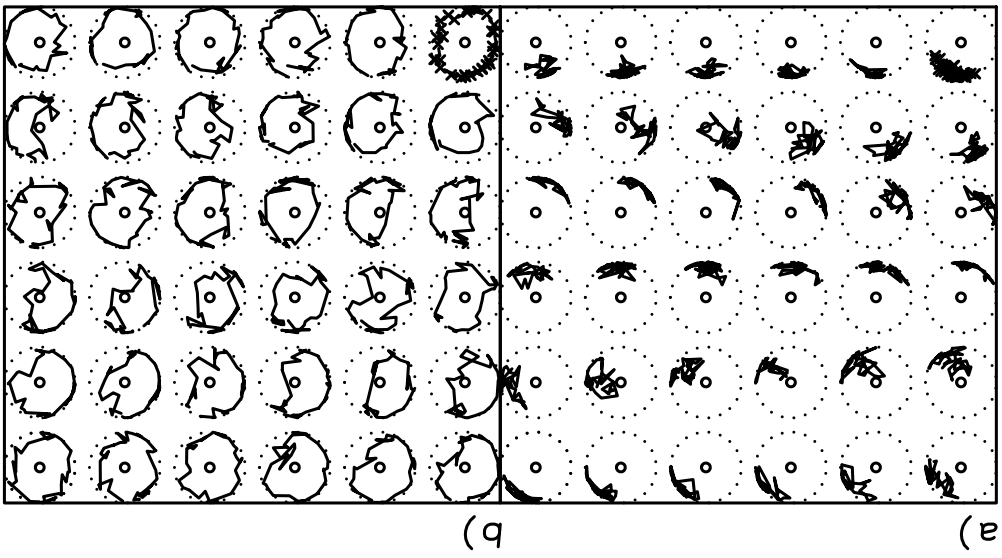




FIG. 2



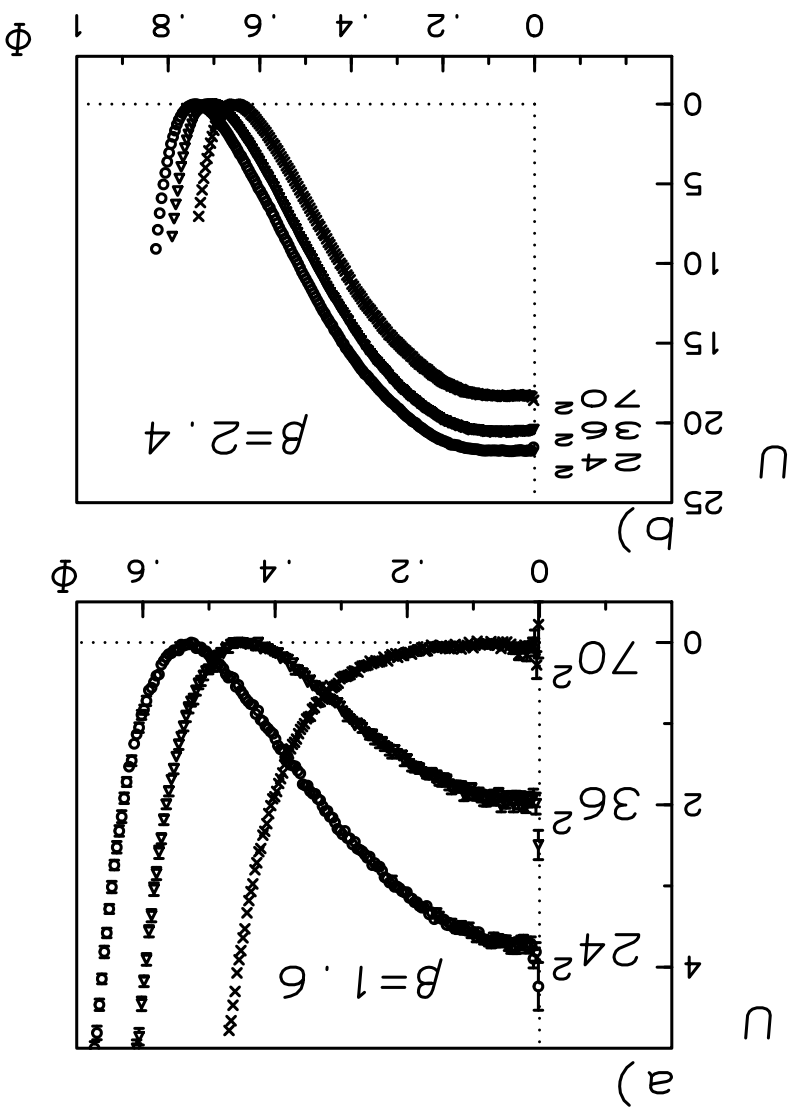


FIG. 3

FIG. 4

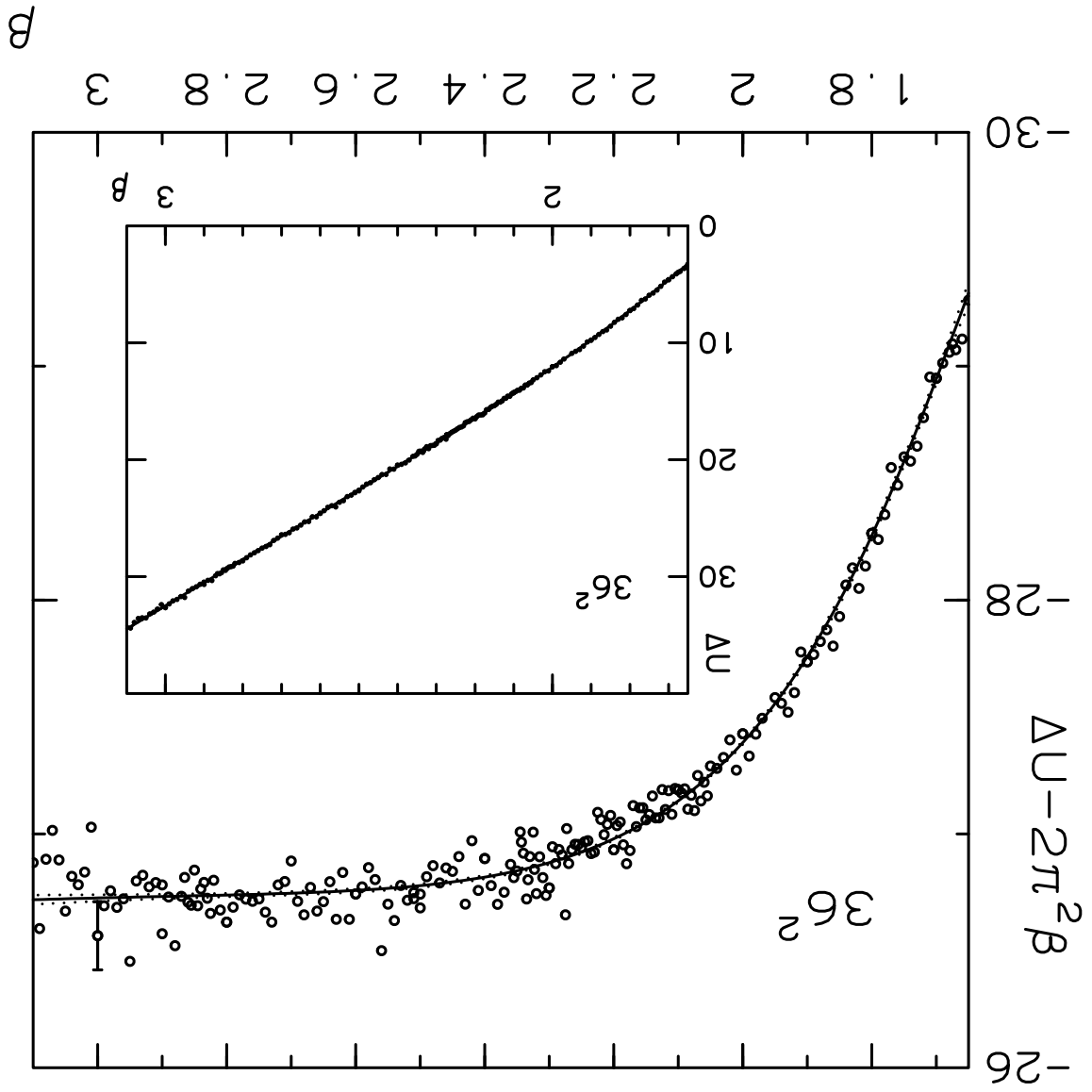


FIG. 5

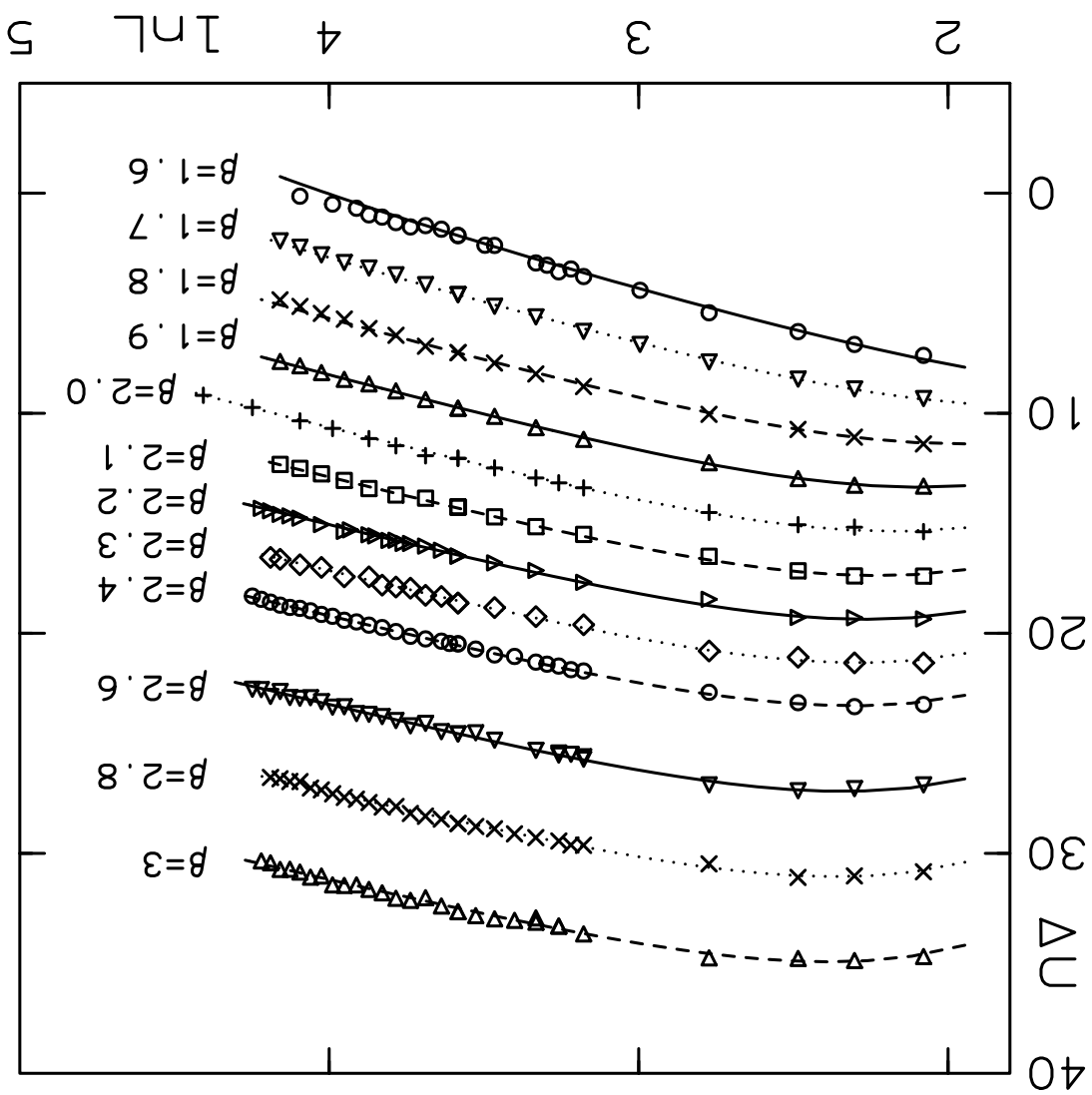
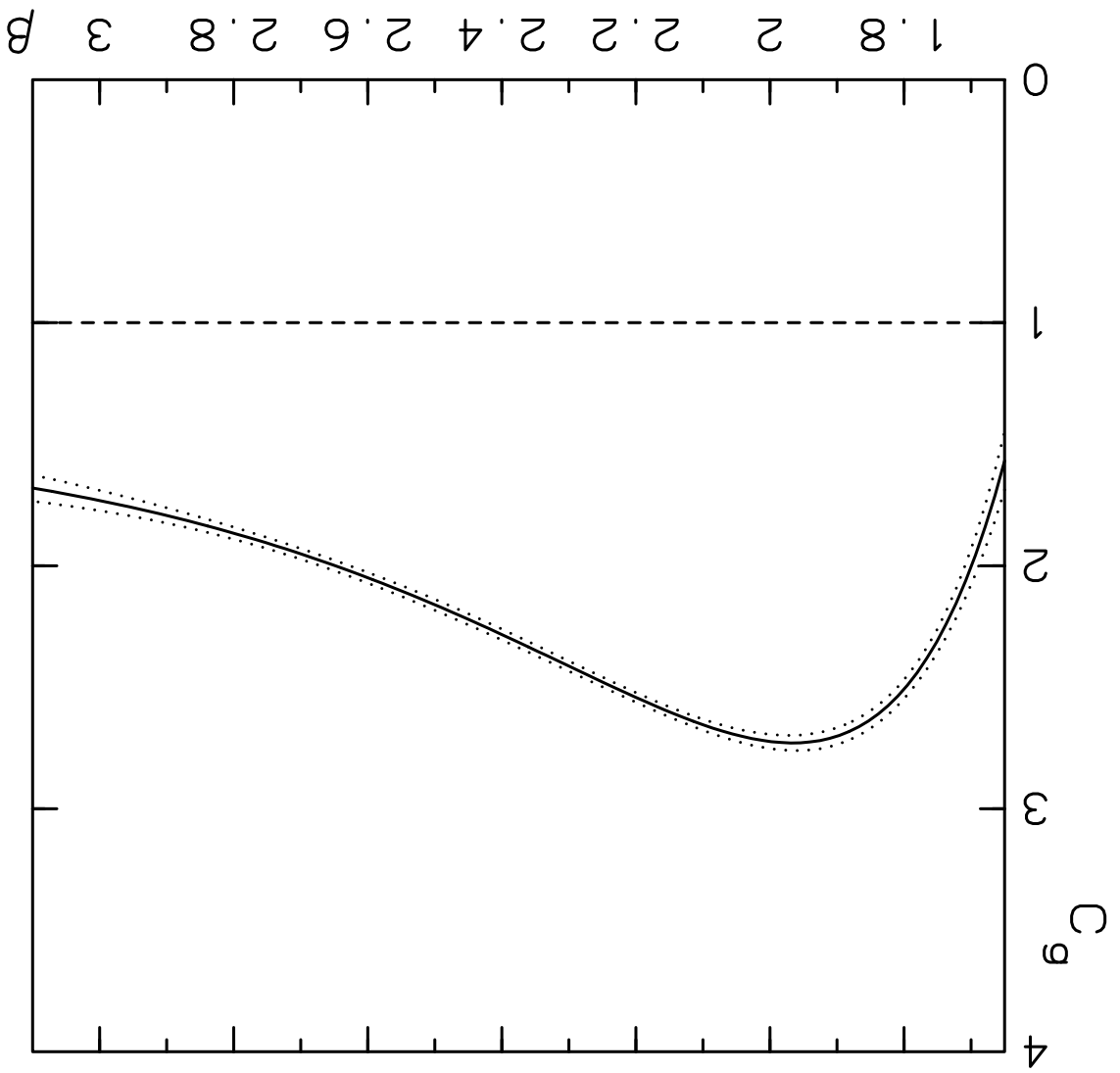


FIG. 6



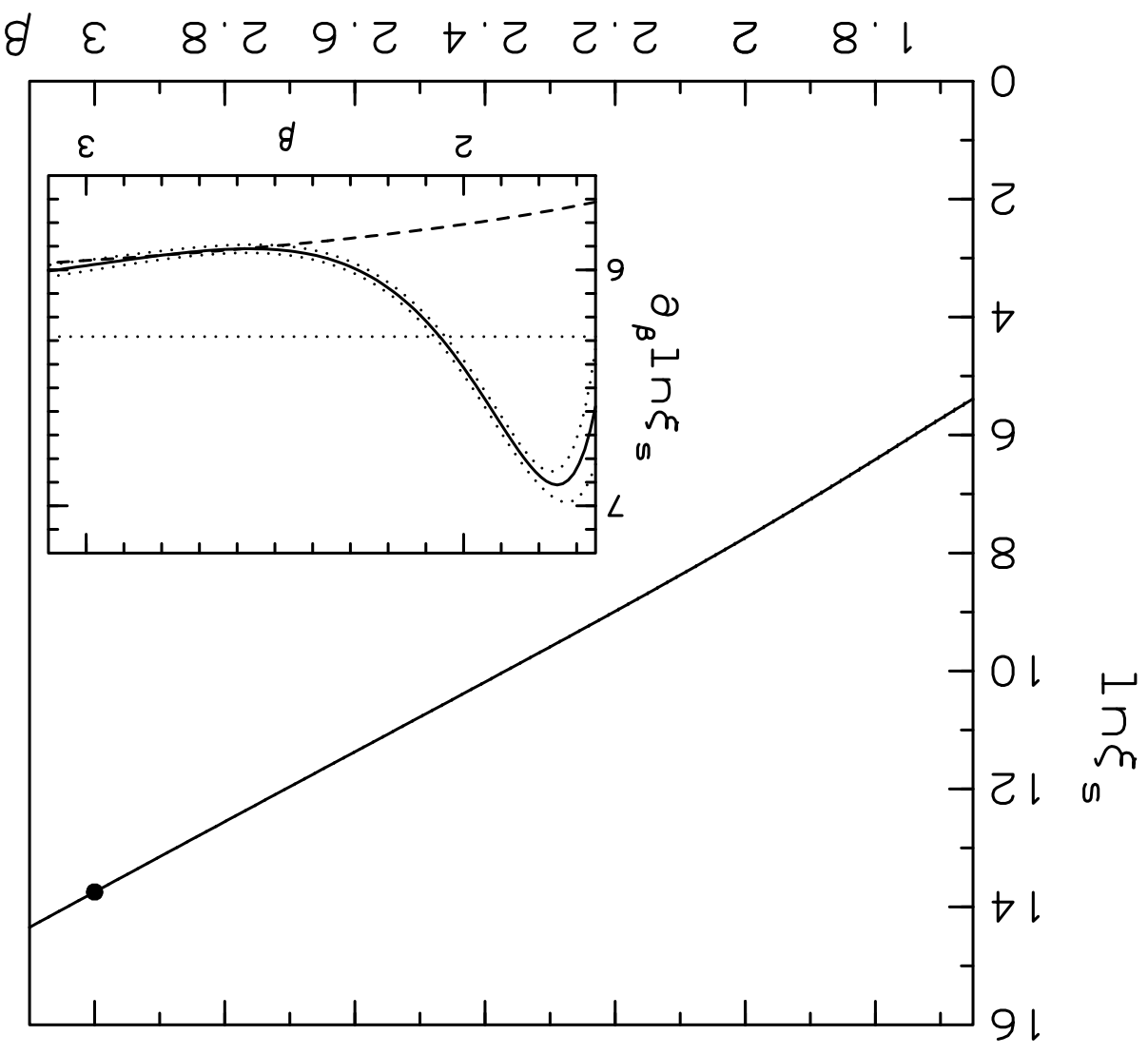


FIG. 7

FIG. 8

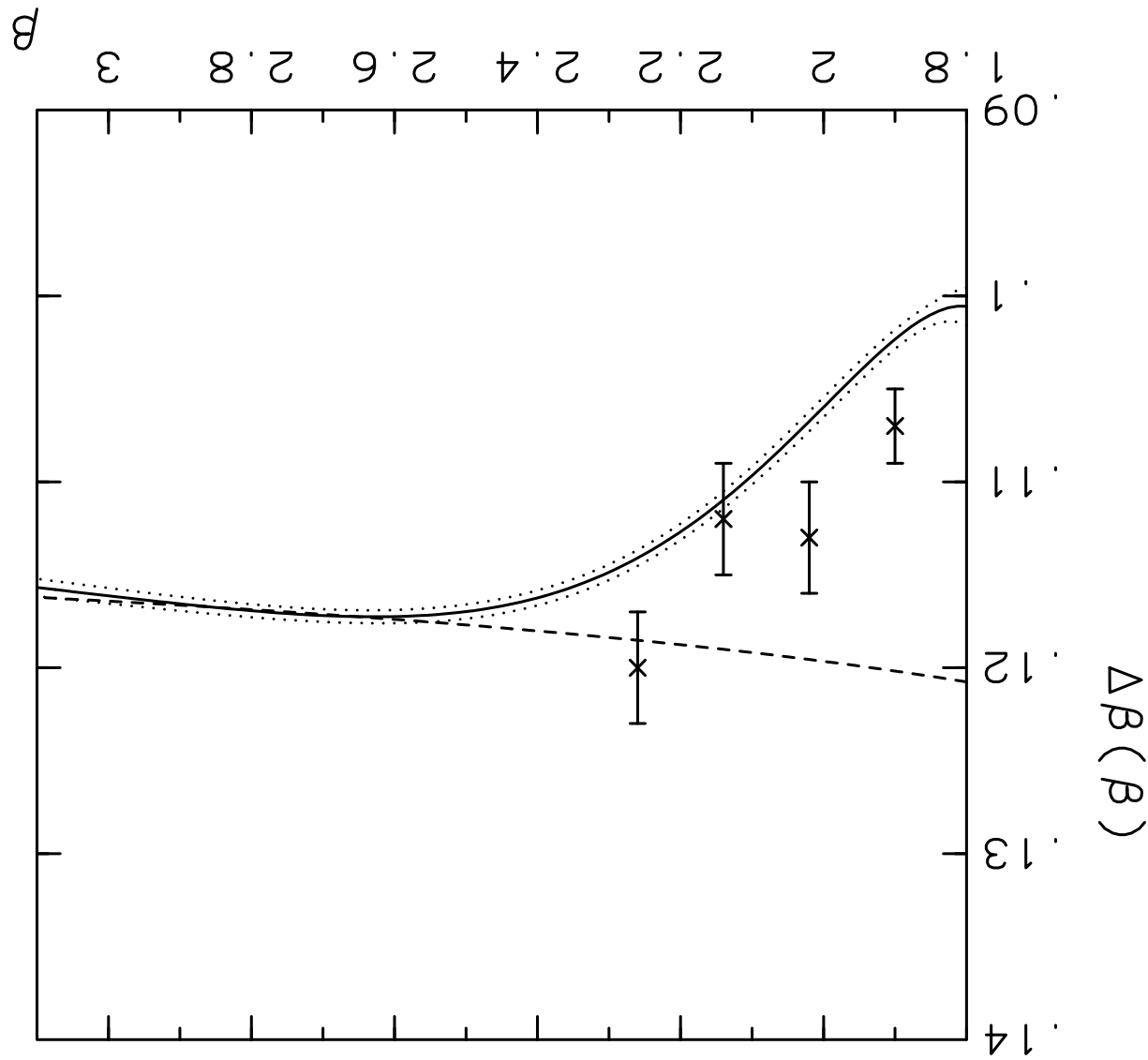


FIG. 9

